Key Points:
- Dissolved black carbon (DBC) concentrations across the global cryosphere are low, with the exception of snow and surface waters near local sources
- Samples collected from the Greenland Ice Sheet were enriched in highly condensed DBC, relative to other samples from the global cryosphere
- DBC composition across the cryosphere is influenced by photodegradative processing and combustion conditions under which it was formed

Correspondence to:
A. L. Khan,
alia.khan@colorado.edu

Dissolved black carbon in the global cryosphere: Concentrations and chemical signatures

Alia L. Khan[1,2] iD, **Sasha Wagner**[3,4] iD, **Rudolf Jaffe**[3], **Peng Xian**[5] iD, **Mark Williams**[6] iD, **Richard Armstrong**[1], and **Diane McKnight**[2] iD

[1]Department of Civil and Environmental Engineering and the Institute of Arctic and Alpine Research, University of Colorado Boulder, Boulder, Colorado, USA, [2]National Snow and Ice Data Center and Cooperative Institute for Research in Environmental Sciences, University of Colorado Boulder, Boulder, Colorado, USA, [3]Southeast Environmental Research Center and Department of Chemistry and Biochemistry, Florida International University, Miami, Florida, USA, [4]Skidaway Institute of Oceanography, Marine Sciences Department, University of Georgia, Savannah, Georgia, USA, [5]Aerosol and Radiation Section of the Marine Meteorology Division, Naval Research Laboratory, Monterey, California, USA, [6]Department of Geography and the Institute of Arctic and Alpine Research, University of Colorado Boulder, Boulder, Colorado, USA

Abstract Black carbon (BC) is derived from the incomplete combustion of biomass and fossil fuels and can enhance glacial recession when deposited on snow and ice surfaces. Here we explore the influence of environmental conditions and the proximity to anthropogenic sources on the concentration and composition of dissolved black carbon (DBC), as measured by benzenepolycaroxylic acid (BPCA) markers, across snow, lakes, and streams from the global cryosphere. Data are presented from Antarctica, the Arctic, and high alpine regions of the Himalayas, Rockies, Andes, and Alps. DBC concentrations spanned from 0.62 µg/L to 170 µg/L. The median and (2.5, 97.5) quantiles in the pristine samples were 1.8 µg/L (0.62, 12), and nonpristine samples were 21 µg/L (1.6, 170). DBC is susceptible to photodegradation when exposed to solar radiation. This process leads to a less condensed BPCA signature. In general, DBC across the data set was composed of less polycondensed DBC. However, DBC from the Greenland Ice Sheet (GRIS) had a highly condensed BPCA molecular signature. This could be due to recent deposition of BC from Canadian wildfires. Variation in DBC appears to be driven by a combination of photochemical processing and the source combustion conditions under which the DBC was formed. Overall, DBC was found to persist across the global cryosphere in both pristine and nonpristine snow and surface waters. The high concentration of DBC measured in supraglacial melt on the GRIS suggests that DBC can be mobilized across ice surfaces. This is significant because these processes may jointly exacerbate surface albedo reduction in the cryosphere.

Plain Language Summary Here we present dissolved black carbon (DBC) results for snow and glacial melt systems in Antarctica, the Arctic, and high alpine regions of the Himalayas, Rockies, Andes, and Alps. Across the global cryosphere, DBC composition appears to be a result of photochemical processes occurring en route in the atmosphere or in situ on the snow or ice surface, as well as the combustion conditions under which the DBC was formed. We show that samples from the Greenland Ice Sheet (GRIS) have a distinct molecular chemical signature, consistent with deposition of BC from Canadian wildfires occurring the week before sampling. The concentration range observed in this global cryosphere study indicates significant amounts of DBC persist in both pristine and human-impacted snow and glacial meltwater. Our results are significant for understanding the controls on meltwater production from glaciers worldwide and the feedbacks between combustion sources, wildfires, and the global cryosphere. Wildfires are predicted to increase due to climate change, and albedo cannibalism is already influencing meltwater generation on the GRIS. Anticipated longer summer melt seasons as a result of climate change may result in longer durations between snowfalls, enhancing exposure of recalcitrant DBC on snow/ice surfaces, which could further exacerbate surface albedo reduction in the cryosphere.

1. Introduction

Many inherent challenges remain in quantifying and predicting melt of polar ice sheets and glaciers. In particular, the complex influence of light-absorbing aerosols is not well understood [*Bond et al.*, 2013]. Biomass burning and fossil fuel combustion are both sources of black carbon (BC) to the cryosphere [*Fellman et al.*, 2015]. Organic matter from these sources can be stored in glaciers for millennia [*Hood et al.*, 2009, 2015; *Stubbins et al.*, 2012a] and mobilized during glacial melting [*Hodson*, 2014]. A study on the

Greenland Ice Sheet (GRIS) attributed two widespread melting events (1889 and 2012) to BC produced from Northern Hemisphere wildfires [*Keegan et al.*, 2014]. This attribution was based on higher BC and ammonia concentrations in ice lenses in firn cores, along with air mass back trajectory analysis; however, direct chemical characterization of the BC was not obtained. Once deposited, BC aerosols can be solubilized and transported in the aqueous phase as dissolved black carbon (DBC) [*Dittmar*, 2008]. In Alaskan glacier rivers, DBC was interpreted as being sourced from atmospheric deposition of anthropogenic combustion products [*Ding et al.*, 2014a]. In Antarctica, DBC from wildfires in preindustrial eras has accumulated over millennia in the saline bottom waters of closed-basin lakes; the DBC in the bottom waters has a more polycondensed chemical signature in comparison to DBC in surface waters susceptible to influence from current local anthropogenic point sources of BC [*Khan et al.*, 2016]. Therefore, atmospheric deposition of both natural and anthropogenic BC aerosols represents an important source of DBC to remote areas of the cryosphere.

DBC is quantified and characterized using the benzenepolycarboxylic acid (BPCA) method, which produces individual BPCA molecular markers upon the oxidation of condensed aromatic structures [*Dittmar*, 2008]. The condensed aromaticity of DBC can be inferred from the relative proportion of produced BPCAs [*Schneider et al.*, 2010; *Abiven et al.*, 2011]. The degree of aromatic condensation for particulate BC is primarily a function of pyrolysis temperature, and links between BPCA composition and pyrogenic source are not always clear [e.g., *Schneider et al.*, 2010; *Mcbeath et al.*, 2013a, 2013b; *Wiedenmeyer et al.*, 2015]. In addition, DBC molecular signatures are altered via photodegradation, either en route or in situ, changing BPCA composition and obscuring potential links to its pyrogenic source [*Schneider et al.*, 2010; *Ziolkowski and Druffel*, 2010; *Stubbins et al.*, 2012b; *Ward et al.*, 2014]. Although BPCA composition cannot be used to directly infer the pyrogenic source of DBC, we can use them to investigate potential biogeochemical drivers of the quality of DBC which persists in cryospheric environments. In this study, we hypothesize that a more condensed DBC signature will be characteristic of samples for sites with freshly deposited BC and limited time for photodegradation, while DBC enrichment in less condensed aromatics will be characteristic for sites where the DBC may have been exposed to solar radiation for long durations of time either in the atmosphere or on the snow/ice surface. In terms of sites with freshly deposited BC, we investigated sites on the GRIS where collection occurred shortly after Canadian wildfires. We also investigated sites where continuous inputs of local anthropogenic sources of BC may lead to a fresher signature. In addition to the GRIS, an area known to be impacted by wildfire-derived pyrogenic carbon, we included other polar regions with high solar exposure, which are exposed to continuous sunlight almost 4 months per year, as well as high-altitude mountain sites. Sampling locations in this study are largely remote, experience extended lengths of sunlight exposure, and receive diverse inputs of atmospheric BC from both natural and anthropogenic combustion sources. As such, our overall hypothesis is that in the cryosphere, degradative processing during DBC transit in the environment, as well as the combustion conditions under which the DBC was formed, are important drivers of the DBC BPCA profile across the cryosphere.

Here we assess variation in DBC content and composition in samples that represent the typical global cryosphere, as well as sites with known local sources of DBC (Figure 1: map). Data are presented from glacial melt systems in Antarctica, the Arctic (GRIS and Svalbard), and high alpine regions of the Himalayas, Rocky Mountains, Andes, and Alps. Snow samples are from the Rocky and Andes Mountains, as well as the Arctic. Samples from the Norwegian Arctic were collected on Svalbard, including around an active coalmine and coal burning power plant, fueling the largest settlement, Longyearbyen. Sites are categorized as "pristine" (*P*; >5 km from a fuel combustion source) and "nonpristine" (NP; <5 km from a fuel combustion source). To support the interpretation of the GRIS results, we determined biomass burning smoke aerosol optical thickness (AOT) and air mass transport from the Navy Aerosol Analysis and Prediction System (NAAPS) over several days in the week before the samples were collected.

2. Methods

Water samples were obtained that represent the diverse aquatic environments of the cryosphere. The lakes and streams sampled include supraglacial systems found on the surface of glaciers, systems fed directly by glacial melt and/or snow melt, as well as proglacial lakes, which form at the tongue of glaciers. There are also surface water ponds included from the McMurdo Dry Valleys (MDVs), including DL-Hoare Pond (DLH Pond), latitude: −77.622901916504, longitude: 162.902999877930, which is adjacent to Lake
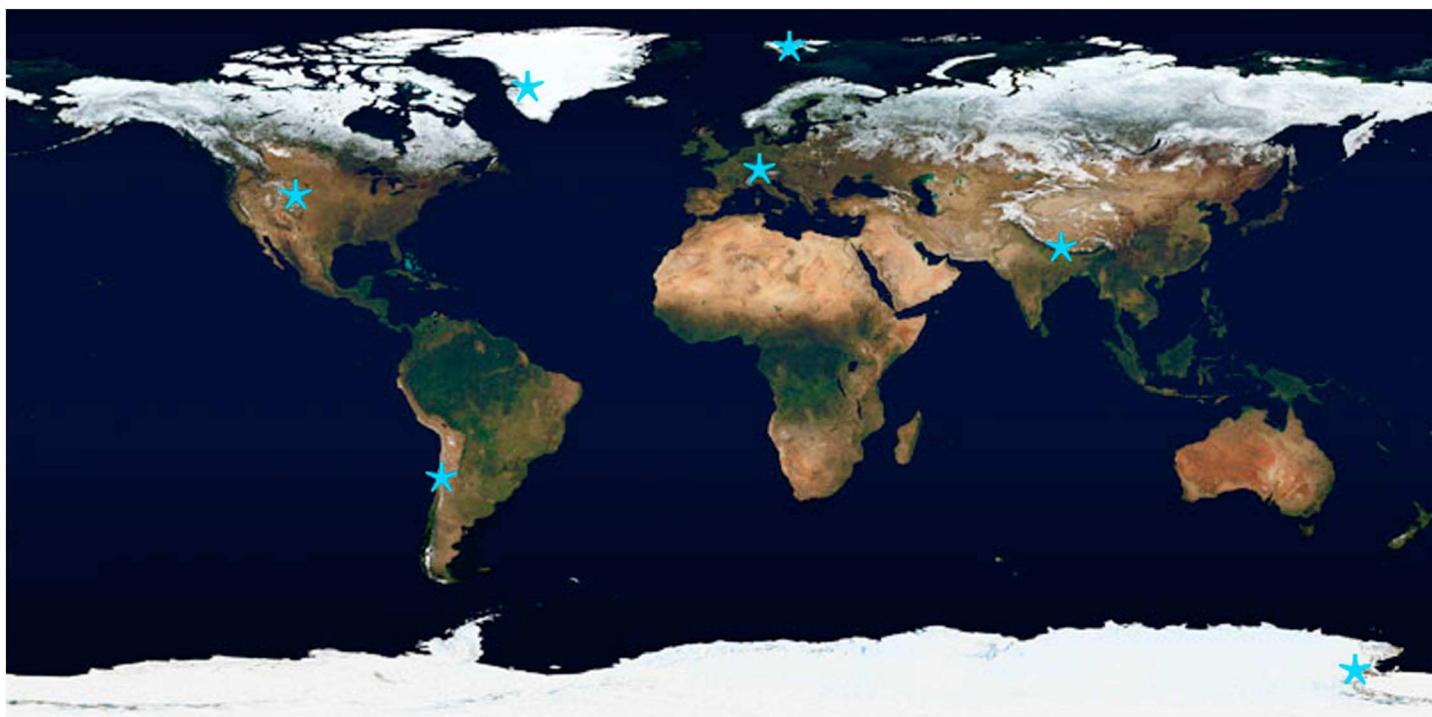
Figure 1. Map of global distribution of sample sites overlaid on a NASA Visible Earth image. Data are presented from glacial melt systems in Antarctica, the Arctic, and the Himalayas. Snow samples are from the Rocky and Andes Mountains, as well as the Arctic.

Hoare: http://www.mcmlter.org/content/dirty-little-hoare-pond. Lake Hoare was named for physicist Ray Hoare, of the eighth Victoria University Expedition (1963–1964). Additional samples were collected at Cape Royds in Antarctica. Regionally, the samples are divided into Arctic, Antarctic, and Alpine. The Arctic data set is mostly composed of samples from the island of Svalbard in the Norwegian Arctic, as well as two samples from the GRIS, one fresh snow and one supraglacial melt. Antarctic samples were collected from the MDV and Cape Royds. Alpine samples are from snow and snowmelt in the Colorado Rocky Mountains, supraglacial melt from the Ngozumba Glacier, the longest glacier in Nepal located in the Gokyo Valley of the Nepalese Himalayas, snow and glacier-fed streams in the central Chilean Andes, and a glacier-fed stream from the Mer de Glace in the French Alps.

Water and snow samples were collected in acid-rinsed and precombusted amber glass bottles or acid-rinsed high-density polyethylene (HDPE) bottles. Snow was melted at room temperature in precleaned acid-rinsed Nalgene buckets. All samples were filtered on precombusted glass fiber filters (Whatman GF/F, pore size: 0.7 μm), acidified to pH = 2 with concentrated HCl (analytical grade), and stored at 4°C until analysis. For all samples, a 60 mL aliquot was poured into acid-rinsed and precombusted amber glass bottles and analyzed for dissolved organic carbon on a Shimadzu TOC-V-CSN with a detection limit of 0.07 mg C/L.

DBC (<0.7 μm) was measured using the BPCA method [*Dittmar*, 2008; *Dittmar et al.*, 2008] and optimization for freshwater DBC [*Ding et al.*, 2014b]. This method is based on the oxidation of polycondensed DBC structures to BPCAs with three to six carboxylic acid groups (B3CA to B6CA). The BPCA method was applied to the dissolved organic matter (DOM) isolated by solid-phase extraction (SPE). First, a SPE technique [*Dittmar*, 2008; *Dittmar et al.*, 2008] was applied to all samples using Bond Elut PPL cartridges, composed of a styrene-divinylbenzene polymer solid phase. SPE efficiency for marine samples is typically ~45% and ~60% in freshwater [*Dittmar et al.*, 2008]. In this study we measured SPE efficiency on eight samples (five Antarctic surface waters (37%, 34%, 46%, 50%, and 67%), a glacier-fed stream from the Andes (34%), and two snow samples (47% and 73%). The average efficiency of these eight samples was 48% ± 15%, with a range from 34% to 73%.

The PPL cartridges were transported frozen to Boulder, CO, and stored in a freezer. The PPL cartridges were transported to Miami, FL, and completely dried under ultrahigh-purity nitrogen gas. The PPL cartridges were then eluted with 10–20 mL of MeOH until the eluent was colorless. Aliquots of MeOH were then

quantitatively transferred to 2 mL glass ampules and evaporated to dryness under a stream of ultrahigh-purity nitrogen. The dried DOM extract was redissolved in concentrated nitric acid (65%) before ampules were sealed and oxidized in sealed glass ampules in a programmable oven for 6 h at 160°C in order to produce BPCAs [*Ding et al.*, 2014b]. They were then dried in a sand bath under ultrahigh-purity nitrogen gas. BPCAs were then redissolved in the mobile phase buffer, separated, and quantified on a Sunfire C18 reversed phase column (3.5 μm, 2.1 × 150 mm; Waters Corporation) by an HPLC system coupled with a photo diode array detector [*Dittmar*, 2008; *Ding et al.*, 2012]. DBC concentrations were calculated from B3CA to B6CA concentrations based on a previously reported algorithm [*Dittmar*, 2008]. B6CA was excluded from BPCA proportion analysis due to its low signal and low resolution in most samples. Analytical replicates were measured in triplicate with <10% standard deviation. Sample duplicates were collected for 5% of the samples and fell within this <10% standard deviation.

The degree of condensed aromaticity of DBC in each sample was estimated based upon the BPCA distribution [*Glaser et al.*, 1998; *Ding et al.*, 2014b] using the ratio of (B3CA + B4CA)/B5CA. Although a complete understanding of all biogeochemical factors that influence BPCA ratios remains elusive, the ratios can be used to provide preliminary assessments of the environmental dynamics of DBC. For instance, photodegradation can significantly alter BPCA composition, reducing the overall condensed aromaticity of the DBC pool once it reaches surface waters [*Stubbins et al.*, 2012b; *Ward et al.*, 2014]. As such, the DBC signature of samples exposed to solar radiation over long durations may indicate extensive photodegradation, resulting in low signals of B6CA. BPCA ratios can also vary significantly with pyrogenic source material and environmental conditions. For example, higher abundance of B5CA + B6CA, indicating more condensed aromatic DBC, has been associated with DBC in wildfire-impacted watersheds [*Wagner et al.*, 2015], whereas DBC solubilized from urban dust has been shoen to be more enriched in B3CA + B4CA (i.e., less polycondensed BC) [*Ding et al.*, 2014a, 2014b]. Although we understand that the source of pyrolized carbon (i.e., fossil fuels or biomass burning) can influence DBC quality, we expect BPCA compositions for the current sample set to be influenced by the atmospheric residence time of the original aerosol BC source and the degree of exposure to solar radiation (Table 1). Thus, we expected to observe lower (B3CA + B4CA)/B5CA ratios when atmospheric transport time was long and/or opportunities for photodegradation were high.

The biomass burning smoke aerosol optical thickness (AOT) data used in this study were obtained from the Navy Aerosol Analysis and Prediction System (NAAPS) reanalysis [*Lynch et al.*, 2016]. NAAPS reanalysis is a decade-long global 1 × 1° and 6-hourly 550 nm AOT reanalysis product, which was recently developed and validated at the Naval Research Laboratory. This reanalysis utilizes a modified version of the NAAPS as its core and assimilates quality-controlled retrievals of AOT from Moderate Resolution Imaging Spectroradiometer (MODIS) on Terra and Aqua and the Multiangle Imaging Spectroradiometer (MISR) on Terra [*Zhang and Reid*, 2006; *Hyer et al.*, 2011; *Shi et al.*, 2014]. NAAPS characterizes anthropogenic and biogenic fine aerosol species (including sulfate and primary and secondary organic aerosols), dust, biomass burning smoke, and sea-salt aerosols. Smoke from biomass burning is derived from near-real-time satellite-based thermal anomaly data used to construct smoke source functions [*Reid et al.*, 2009], with additional orbital corrections on MODIS-based emissions and regional tunings. The reanalyzed fine- and coarse-mode AOT at 550 nm is shown to have good agreement with the ground-based global-scale Sun photometer network Aerosol Robotic Network AOTs [*Holben et al.*, 1998]. Figure 3 is a series of snapshots at 18Z showing wildfire-related smoke AOT at 550 nm between 18 and 21 June 2014 at 550 nm.

3. Results and Discussion

As expected, pristine sites had lower median and (2.5, 97.5) quantiles of DBC concentrations (1.8 μg/L (0.62, 12)) than nonpristine sites (21 μg/L (1.6, 170)). In particular, pristine snow samples exhibited low DBC concentrations (1.8 μg/L (1.3, 10)). The median (B3CA + B4CA)/B5CA ratio for pristine samples from snow was 3 (1, 27) (Table 1 and Figure 2). The remote pristine snow/surface hoar sample from the GRIS had a distinct composition compared to the rest of the data set, containing high levels of B5CA and a ratio of 0.3, below the 2.5% quantile. Similar to the glaciers of Antarctica [*Khan et al.*, 2016], the only potential source of BC to the GRIS is long-range atmospheric transport. The GRIS sample was collected in late June 2014, as wildfires blazed across the Canadian Arctic. As shown by the reanalysis from the NAAPS model, continuous smoke activities occurred over the northwest of Canada between 18 and 21 June 2014 and were transported eastward to the

Table 1. Samples Grouped by Pristine and Nonpristine in Ascending Order of (B3CA + B4CA)/B5CA Ratio[a]

	(B3CA + B4CA)/B5CA	DBC (µg/L)	DOC (mg/L)	%DOC of DBC	Region	Medium	Geography
Pristine Snow Sample							
GRIS snow/surface hoar	0.82	1.76	0.67	0.003	GRIS	Snow <1, hoar >5 days	Arctic
Chilean Andes Snow-ET	3.0	1.80	0.83	0.002	Andes	Snow <2 days	Alpine
Niwot Ridge B	3.0	8.93	nd	nd	Rockies	Snow <1 day	Alpine
San Francisco Glacier Snow	3.4	1.44	0.36	0.004	Andes	Snow <2 days	Alpine
WoodFjorden, Svalbard	4.2	1.26	0.54	0.002	Svalbard	Snow <2 days	Arctic
Larsbren	6.3	1.63	0.39	0.004	Svalbard	Snow >5 days	Arctic
Storm Peak Lab	17	9.65	nd	nd	Rockies	Snow >3 days	Alpine
Niwot Ridge A	27	9.27	nd	nd	Rockies	Snow >3 days	Alpine
Pristine Meltwater Samples							
GRIS supraglacial melt	0.32	12.4	0.14	0.088	GRIS	Supraglacial melt	Arctic
Mer de Glace, Chamonix	1.8	1.51	4.13	0.000	Alps	Glacial stream	Alpine
Bano Morales Stream	1.9	6.12	0.50	0.012	Andes	Glacial stream	Alpine
Lake Joyce 7 m[b]	2.5	2.67	0.50	0.005	Antarctic	Lake	Antarctic
Alatna Pond	3.2	3.60	1.00	0.004	Antarctic	Surface water	Antarctic
Lake Bonney East Lobe 5 m	3.6	1.44	0.40	0.004	Antarctic	Lake	Antarctic
Von Guerrard Stream[b]	3.6	0.89	0.63	0.001	Antarctic	Glacial stream	Antarctic
Ngozumba Glacier, Nepal	3.7	1.05	0.10	0.010	Himalayas	Supraglacial lake	Alpine
Ngozumba Glacier, Nepal	3.8	0.62	0.12	0.005	Himalayas	Supraglacial lake	Alpine
Alaskan Glacial Rivers[c]	4.3	0.53 ± 0.09	0.010 ± 0.004	1.9 ± 0.6	Alaska	Glacial river	Arctic
Lake Bonney West Lobe 5 m[b]	5.4	1.22	0.40	0.003	Antarctic	Lake	Antarctic
Green Lake 4, Colorado	5.4	4.40	nd	nd	Rockies	Lake	Alpine
Ngozumba Glacier, Nepal	6.3	1.54	0.12	0.012	Himalayas	Supraglacial lake	Alpine
Ngozumba Glacier, Nepal	6.7	1.94	0.40	0.005	Himalayas	Supraglacial lake	Alpine
Ngozumba Glacier, Nepal	6.8	1.39	0.83	0.002	Himalayas	Supraglacial Lake	Alpine
Nonpristine Snow							
Mine 7	3.3	71.4	1.03	0.070	Svalbard	Snow >5 days	Arctic
Upwind of the Mine	7.7	2.36	5.43	0.000	Svalbard	Snow >5 days	Arctic
Next to Coal Power Plant	17	6.84	0.32	0.021	Svalbard	Snow >5 days	Arctic
Upper Snowmobile Track	43	44.4	4.68	0.009	Svalbard	Snow >5 days	Arctic
Lower Snowmobile Track	59	21.6	0.54	0.040	Svalbard	Snow >5 days	Arctic
Nonpristine Meltwater							
High Park Fire PNF0714[d]	1.3	177	2.97	0.06	Rockies	Terrestrial stream	Alpine
Marble Point	1.5	33.6	4.23	0.008	Antarctic	Surface water	Antarctic
Clear Lake	2.2	47.3	4.30	0.011	Antarctic	Surface water	Antarctic
Lake Fryxell 5 m	2.2	8.28	1.80	0.005	Antarctic	Lake	Antarctic
DLH Pond	3.1	14.0	2.30	0.006	Antarctic	Surface water	Antarctic
Pony Lake	3.4	170	19.0	0.009	Antarctic	Surface water	Antarctic
Longyear River	3.5	4.68	5.83	0.001	Svalbard	Glacial stream	Arctic
Longyearbyen Fjord Water	4.3	20.5	0.33	0.062	Svalbard	Ocean	Arctic

[a]A lower ratio is more indicative of wildfire-derived DBC, and a higher ratio is more indicative of fossil fuel combustion and/or photodegradation.
[b]From *Khan et al.* [2016].
[c]From *Ding et al.* [2014a, 2014b].
[d]From *Wagner et al.* [2015].

western region of the GRIS (Figure 3). Fresh aerosols from these fires, which appear to have been transported to the western region of the GRIS, would have remained in the surface hoar with limited time for photodegradation prior to sample collection and provide an explanation for the highly condensed aromatic DBC signal observed for this sample. The other most remote pristine snow sample was from Svalbard, which had a DBC concentration of 1.1 µg/L and BPCA ratio of 4. This sample was collected in Woodfjorden, which is several hundred kilometers from the closest town, thus only impacted by atmospheric long-range transport.

Pristine snow samples from the Rocky Mountains had similar DBC concentrations, from 8.9 to 9.7 µg/L, but the (B3CA + B4CA)/B5CA ratios ranged from 3 to 27. Two of the pristine snow samples yielded (B3CA + B4CA)/B5CA ratios higher than the Woodfjorden sample, 4.2. The (B3CA + B4CA)/B5CA ratio was 17 at Storm Peak Lab in Northern Colorado and 27 at Niwot Ridge in central Colorado (Table 1), suggesting that the BC in these remote Colorado samples is less condensed than the remote sample from Svalbard, which may be indicative of more photodegradation of DBC at the Colorado sites prior to sample
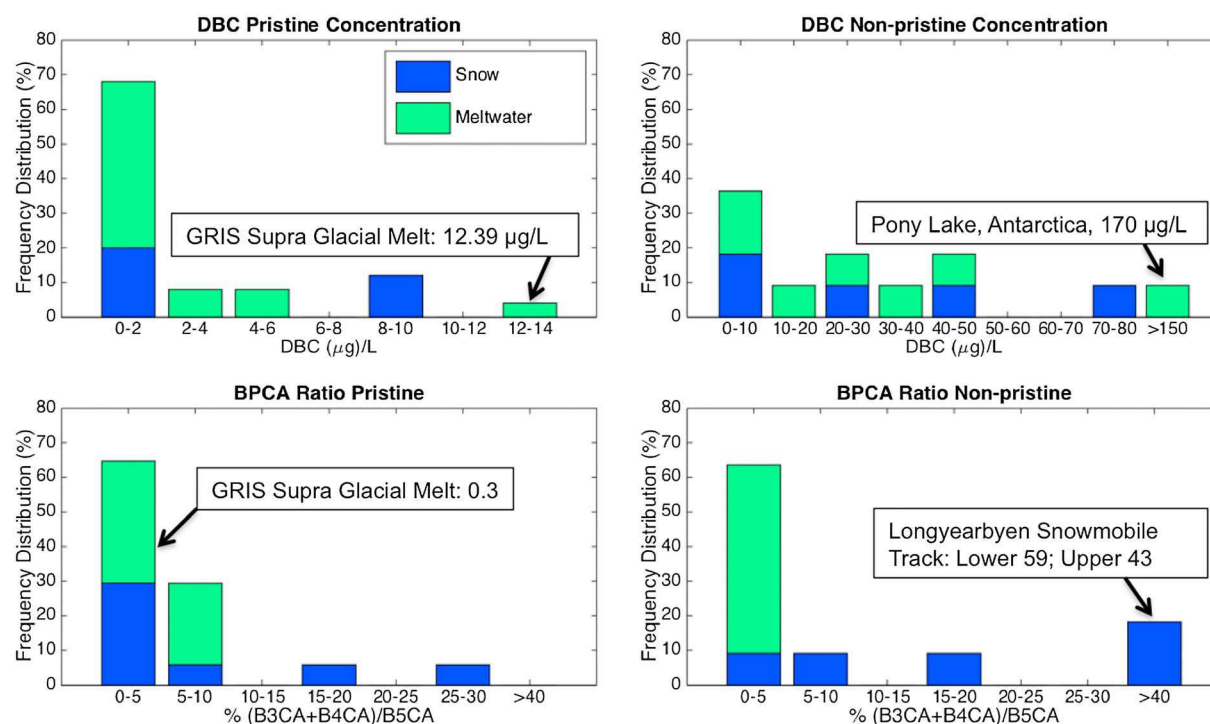
Figure 2. Frequency distribution of pristine and nonpristine snow and meltwater samples from unpublished values in Table 1. Meltwater samples are composed of both snow and ice melt. Note that the maximum *x* axis value for DBC pristine concentration is 14 μg/L versus 150 μg/L for DBC nonpristine concentration.

collection, or a different pyrolized source. These two samples were aged snow samples and exposed to solar radiation longer than the Woodfjorden sample (Table 1). In contrast, a fresh snow sample from a similar location in the Rocky Mountains only yielded a (B3CA + B4CA)/B5CA ratio of 3. The DBC in this fresh snow sample had limited time for photodegradation, which may result in the less condensed BPCA ratio, relative to the aged snow samples from the Rocky Mountains. Again, these sites are >5 km away from known point sources so the enrichment in less condensed DBC may be related to accumulated solar exposure from the time since snow deposition to the time of sample collection and/or the long-range transport of fossil fuel-derived soot particles, which have been found on remote glaciers [*Stubbins et al.*, 2012a; *Ding et al.*, 2014a].

Median DBC concentrations were higher in nonpristine snow samples (14 μg/L (1.6, 71)) than pristine snow samples (1.8 μg/L (1.3, 10)). Furthermore, the median (B3CA + B4CA)/B5CA ratio for nonpristine samples from snow was much higher than pristine snow samples, 12 (3, 59) and 3 (1, 27), respectively (Table 1 and Figure 2). The highest DBC concentrations in snow were found in samples collected from Longyearbyen, Svalbard, next to an active coalmine (71 μg/L), a coal burning power plant (6.8 μg/L), and along the primary Longyearbren snowmobile track (22 μg/L upper track; 44 μg/L lower track), which receives continuous inputs of fresh anthropogenic BC. In contrast to our hypothesis that continuous inputs would result in a signature less indicative to photodegradation, these samples also feature the highest (B3CA + B4CA)/B5CA ratios, with the snow next to the coal burning power plant featuring a ratio of 17, and even higher ratios along the snow-mobile track (43 upper track; 59 lower track).

Pristine meltwaters had low median DBC concentrations (1.7 μg/L (0.6, 12)), similar to the pristine snow samples (1.8 μg/L (1.3, 10)). The median (B3CA + B4CA)/B5CA ratio for pristine meltwaters, 4 (0.3, 7) (Table 1 and Figure 2), was marginally higher than for pristine snow samples, 3 (1, 27). In contrast to the Nepal meltwaters, the GRIS supraglacial meltwater had a high concentration of DBC (12.4 μg/L) corresponding to the 97.5% quantile. In addition, the GRIS meltwater had a similar low ratio of (B3CA + B4CA)/B5CA to the GRIS snow/surface hoar sample. These BPCA ratios (0.3 and 0.8, respectively) were the lowest in this data set and are lower than the previously reported ratios from terrestrial rivers impacted by wildfires [*Wagner et al.*, 2015]. As noted previously, these low ratios likely reflect fresh and recent BC deposition sourced from Canadian Arctic wildfires (Figure 3). The higher DBC concentration compared to the Nepal supraglacial waters
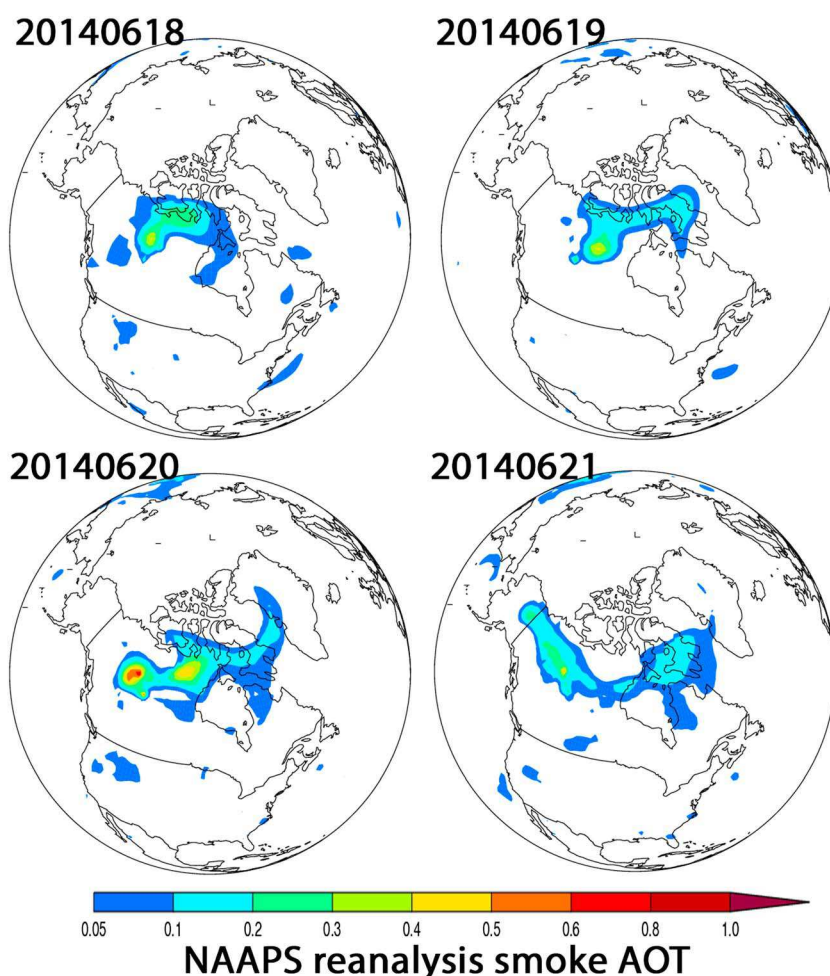
Figure 3. Smoke aerosol optical thickness (AOT) reanalysis at 18Z from the Navy Aerosol Analysis and Prediction System (NAAPS) between 18 and 21 June 2014 shows that wildfire aerosols were transported from the Canadian Arctic to the western region of Greenland Ice Sheet in June 2014. The color bar is atmospheric total column smoke aerosol optical thickness (AOT) at 550 nm, which is unitless.

could reflect not only the substantial long-range wildfire inputs but also the large surface area of the GRIS, which may provide a larger supraglacial catchment for accumulation and transport of DBC to the ablation area where the sample was collected. Further, the high DBC in the GRIS meltwater provides support to the potential positive feedback proposed by *Keegan et al.* [2014] whereby DBC-enriched meltwater is retained as refrozen ice layers in the snowpack and enhances future melting.

Meltwater from supraglacial lakes on the Ngozumba Glacier in Nepal, located at ~5000 m, had the lowest DBC concentrations (average of five samples, 1.3 ± 0.49 µg/L) of all meltwater samples. The ratio of these samples was also composed of less condensed DBC, with an average ratio of 5, than supraglacial melt from the GRIS which was composed of highly condensed DBC and had a ratio of 0.3. Although no nearby snow samples were obtained for direct comparison, these low values from the Ngozumba Glacier may be associated with heavy glacial debris coverage in the majority of the ablation region. The debris cover, when thick enough, provides insulation from glacial melt [*Pratap et al.*, 2015] and may reduce supraglacial meltwater generation, along with transport and accumulation of DBC. Although these lakes form an ice cover from about November to March, in the summer they receive large solar radiation inputs, enhanced by the high altitude, which could drive photodegradation of DBC. The less condensed DBC signature could also suggest different combustion sources of DBC between these sampling locations.

Similar to the observations for snow and ice, nonpristine meltwaters had higher median DBC concentrations, (27 µg/L (4.7, 170)) than pristine meltwaters (1.7 µg/L (0.6, 12)). Closed-basin nonpristine Antarctic surface

waters, such as DLH Pond, Marble Point Pond, Clear Lake, and Pony Lake, contained high concentrations of DBC ranging from 14 to 170, μg/L. These lakes are located near active point sources of fossil fuel combustion, such as helicopter flight paths and fueling stations, and exhibited elevated DBC concentrations relative to snow and meltwater. Because these surface water ponds have no outflowing streams, any DBC deposited in the systems will remain and accumulate for millennia, similar to the MDV lakes [*Khan et al.*, 2016], or may be photodegraded. The BPCA ratio of these four nonpristine Antarctic surface waters ranged from 2 to 3. Similarly, the BPCA ratios for Longyear River and Adventfjord ocean water in the Norwegian Arctic, both located near the town of Longyearbyen and the local coal burning power plant, were both 4. Such elevated DBC concentrations and BPCA ratios suggest that site proximity to continuous inputs from these particular anthropogenic sources results in high concentrations of less condensed DBC and that long-term photooxidation may not be the only cause of less condensed DBC in the cryosphere.

4. Conclusions

This study reveals that within the cryosphere, DBC concentrations and composition are widely variable. Regionally, concentration differences exist between remote-pristine sites and those near combustion point sources. Overall, these data support our hypothesis that DBC in the cryosphere that is exposed to longer durations of solar radiation results in less condensed DBC due to photodegradation. Additionally, sites in the cryosphere receiving fresh BC from wildfires, such as on the GRIS where aerosols were deposited directly from Canadian Arctic wildfires, consist of more condensed DBC. This signature of the DBC from the GRIS was distinct from the sites which receive continuous inputs from local anthropogenic sources of BC, such as along the heavily used snowmobile track in Svalbard, as well as sites which have prolonged sunlight exposure, thus enhancing effects of photodegradation.

While the influence of wildfire inputs throughout the cryosphere may be important regionally, as observed in the samples from the GRIS, the intense solar exposure in high alpine and polar regions, and the characteristics of some anthropogenic combustion sources subject to solar exposure during long-range atmospherics transport [*Cooke and Wilson*, 1996], may cause the similarity in DBC composition observed throughout the rest of the global cryosphere data set. This includes photodegradation of background levels of wildfire-derived BC, which may also contribute to B3 + 4CA enrichment in the cryosphere [*Stubbins et al.*, 2012b; *Ward et al.*, 2014]. As such, the influence of photodegradation may sometimes be "overwhelmed" by discrete wildfire sources, which likely account for DBC composition of the GRIS samples. Although the current data set allowed for preliminary assessments of contributions to and persistence of DBC in the cryosphere, the observed variability of DBC composition is likely derived from a combination of biogeochemical processes in the environment and different pyrogenic sources.

Previously reported accumulation of millennia old DBC in Antarctic lakes [*Khan et al.*, 2016] suggests that DBC is recalcitrant in the cryosphere. The ranges of concentrations observed in this diverse data set of DBC from the global cryosphere indicate that relatively high DBC concentrations persist in both pristine and nonpristine Arctic and Antarctic snow and surface waters. The relatively high concentration of DBC measured in one supraglacial stream on the GRIS may suggest that DBC can be mobilized across ice surfaces. Wildfires are predicted to increase due to climate change [*Flannigan et al.*, 2009], and albedo cannibalism is already influencing meltwater generation on the GRIS [*Tedesco et al.*, 2015]. Anticipated longer summer melt seasons as a result of climate change may result in longer durations between snowfalls, enhancing exposure of recalcitrant DBC on snow/ice surfaces, which could further exacerbate surface albedo reduction in the cryosphere.

References

Abiven, S., P. Hengartner, M. P. W. Schneider, N. Singh, and M. W. I. Schmidt (2011), Pyrogenic carbon soluble fraction is larger and more aromatic in aged charcoal than in fresh charcoal, *Soil Biol. Biochem.*, *43*(7), 1615–1617, doi:10.1016/j.soilbio.2011.03.027.

Bond, T. C., et al. (2013), Bounding the role of black carbon in the climate system: A scientific assessment, *J. Geophys. Res. Atmos.*, *118*, 5380–5552, doi:10.1002/jgrd.50171.

Cooke, W. F., and J. J. N. Wilson (1996), A global black carbon aerosol model, *J. Geophys. Res.*, *101*(D14), 19,395–19,409, doi:10.1029/96JD00671.

Ding, Y., Y. Yamashita, W. K. Dodds, and R. Jaffé (2012), Dissolved black carbon in grassland streams: Is there an effect of recent fire history?, *Chemosphere*, *90*(10), 2557–2562, doi:10.1016/j.chemosphere.2012.10.098.

Ding, Y., Y. Yamashita, J. Jones, and R. Jaffe (2014a), Dissolved black carbon in boreal forest and glacial rivers of central Alaska: Assessment of biomass burning versus anthropogenic sources, *Biogeochemistry*, *123*, 15–25, doi:10.1007/s10533-014-0050-7.

Ding, Y., K. M. Cawley, C. N. da Cunha, and R. Jaffé (2014b), Environmental dynamics of dissolved black carbon in wetlands, *Biogeochemistry*, *119*, 259–273, doi:10.1007/s10533-014-9964-3.

Dittmar, T. (2008), The molecular level determination of black carbon in marine dissolved organic matter, *Org. Geochem.*, *39*(4), 396–407, doi:10.1016/j.orggeochem.2008.01.015.

Dittmar, T., B. Koch, N. Hertkorn, and G. Kattner (2008), A simple and efficient method for the solid-phase extraction of dissolved organic matter (SPE-DOM) from seawater, *Limnol. Oceanogr. Methods*, *6*, 230–235, doi:10.4319/lom.2008.6.230.

Fellman, J. B., E. Hood, P. A. Raymond, A. Stubbins, and R. G. M. Spencer (2015), Spatial variation in the origin of dissolved organic carbon in snow on the Juneau icefield, Southeast Alaska, *Environ. Sci. Technol.*, 150908131727005, doi:10.1021/acs.est.5b02685.

Flannigan, M., B. Stocks, M. Turetsky, and M. Wotton (2009), Impacts of climate change on fire activity and fire management in the circumboreal forest, *Glob. Chang. Biol.*, *15*(3), 549–560, doi:10.1111/j.1365-2486.2008.01660.x.

Glaser, B., L. Haumaier, G. Guggenberger, and W. Zech (1998), Black carbon in soils: The use of benzenecarboxylic acids as specific markers, *Org. Geochem.*, *29*(4), 811–819, doi:10.1016/S0146-6380(98)00194-6.

Hodson, A. J. (2014), Understanding the dynamics of black carbon and associated contaminants in glacial systems, *Wiley Interdiscip. Rev. Water*, *1*(April), 141–149, doi:10.1002/wat2.1016.

Holben, B. N., et al. (1998), AERONET—A federated instrument network and data archive for aerosol characterization, *Remote Sens. Environ.*, *4257*(98).

Hood, E., J. Fellman, R. G. M. Spencer, P. J. Hernes, R. Edwards, D. D'Amore, and D. Scott (2009), Glaciers as a source of ancient and labile organic matter to the marine environment, *Nature*, *462*(7276), 1044–1047, doi:10.1038/nature08580.

Hood, E., T. J. Battin, J. Fellman, S. O'Neel, and R. G. M. Spencer (2015), Storage and release of organic carbon from glaciers and ice sheets, *Nat. Geosci.*, *8*(2), 1–6, doi:10.1038/ngeo2331.

Hyer, E. J., J. S. Reid, and J. Zhang (2011), An over-land aerosol optical depth data set for data assimilation by filtering, correction, and aggregation of MODIS Collection 5 optical depth retrievals, *Atmos. Meas. Tech.*, *4*, 379–408, doi:10.5194/amt-4-379-2011.

Keegan, K. M., M. R. Albert, J. R. Mcconnell, and I. Baker (2014), Climate change and forest fires synergistically drive widespread melt events of the Greenland Ice Sheet, *Proc. Natl. Acad. Sci. U. S. A.*, *111*, 7964–7967, doi:10.1073/pnas.1405397111.

Khan, A. L., R. Jaffé, Y. Ding, and D. M. McKnight (2016), Dissolved black carbon in Antarctic lakes: Chemical signatures of past and present sources, *Geophys. Res. Lett.*, *43*, 5750–5757, doi:10.1002/2016GL068609.

Lynch, P., et al. (2016), An 11-year global gridded aerosol optical thickness reanalysis (v1. 0) for atmospheric and climate sciences, *Geosci. Model Dev.*, *9*, 1489–1522, doi:10.5194/gmd-9-1489-2016.

Mcbeath, A. V., R. J. Smernik, and E. S. Krull (2013a), Organic geochemistry: A demonstration of the high variability of chars produced from wood in bushfires, *Org. Geochem.*, *55*, 38–44, doi:10.1016/j.orggeochem.2012.11.006.

Mcbeath, A. V., R. J. Smernik, E. S. Krull, and J. Lehmann (2013b), ScienceDirect: The influence of feedstock and production temperature on biochar carbon chemistry—A solid-state ^{13}C NMR study, *Biomass Bioenergy*, *60*, 121–129, doi:10.1016/j.biombioe.2013.11.002.

Pratap, B., D. P. Dobhal, M. Mehta, and R. Bhambri (2015), Influence of debris cover and altitude on glacier surface melting: A case study on Dokriani Glacier, central Himalaya, India, *Ann. Glaciol.*, *56*(70), 9–16, doi:10.3189/2015AoG70A971.

Reid, J. S., et al. (2009), Global monitoring and forecasting of biomass-burning smoke: Description of and lessons from the Fire Locating and Modeling of Burning Emissions (FLAMBE) program, *IEEE J. Sel. Top. Appl. Earth Obs. Remote Sens.*, *2*(3), 144–162.

Schneider, M. P. W., M. Hilf, U. F. Vogt, and M. W. I. Schmidt (2010), The benzene polycarboxylic acid (BPCA) pattern of wood pyrolyzed between 200°C and 1000°C, *Org. Geochem.*, *41*(10), 1082–1088, doi:10.1016/j.orggeochem.2010.07.001.

Shi, Y., J. Zhang, J. S. Reid, B. Liu, and E. J. Hyer (2014), Critical evaluation of cloud contamination in the MISR aerosol products using MODIS cloud mask products, *Atmos. Meas. Tech. Discuss.*, 1791–1801, doi:10.5194/amt-7-1791-2014.

Stubbins, A., et al. (2012a), Anthropogenic aerosols as a source of ancient dissolved organic matter in glaciers, *Nat. Geosci.*, *5*(3), 198–201, doi:10.1038/ngeo1403.

Stubbins, A., J. Niggemann, and T. Dittmar (2012b), Photo-lability of deep ocean dissolved black carbon, *Biogeosciences*, *9*(2002), 1661–1670, doi:10.5194/bg-9-1661-2012.

Tedesco, M., S. Doherty, X. Fettweis, P. Alexander, J. Jeyaratnam, E. Noble, and J. Stroeve (2015), The darkening of the Greenland ice sheet: Trends, drivers and projections (1981–2100), *Cryosphere Discuss.*, *9*(5), 5595–5645, doi:10.5194/tcd-9-5595-2015.

Wagner, S., K. M. Cawley, F. L. Rosario-Ortiz, and R. Jaffé (2015), In-stream sources and links between particulate and dissolved black carbon following a wildfire, *Biogeochemistry*, *124*, 145–161, doi:10.1007/s10533-015-0088-1.

Ward, C. P., R. L. Sleighter, P. G. Hatcher, and R. M. Cory (2014), Insights into the complete and partial photooxidation of black carbon in surface waters, *Environ. Sci.: Processes Impacts*, *16*(4), 721–731, doi:10.1039/c3em00597f.

Wiedenmeyer, M., et al. (2015), Aromaticity and degree of aromatic condensation of char, *Org. Geochem.*, *78*, 135–143, doi:10.1016/j.orggeochem.2014.10.002.

Zhang, J., and J. S. Reid (2006), MODIS aerosol product analysis for data assimilation: Assessment of over-ocean level 2 aerosol optical thickness retrievals, *J. Geophys. Res.*, *111*, D22207, doi:10.1029/2005JD006898.

Ziolkowski, L. A., and E. R. M. Druffel (2010), Aged black carbon identified in marine dissolved organic carbon, *Geophys. Res. Lett.*, *37*, L16601, doi:10.1029/2010GL043963.